Baryon Stopping as a New Probe of Geometric Scaling

Yacine Mehtar-Tani and Georg Wolschin

Institut für Theoretische Physik der Universität Heidelberg, Philosophenweg 16, D-69120 Heidelberg, Germany

(Received 24 September 2008; revised manuscript received 28 March 2009; published 6 May 2009)

We suggest using net-baryon rapidity distributions in central relativistic heavy-ion collisions at energies reached at the CERN Super Proton Synchrotron, BNL Relativistic Heavy-Ion Collider (RHIC), and CERN LHC in order to probe saturation physics. Within the color glass condensate framework based on small-coupling QCD, net-baryon rapidity distributions are shown to exhibit geometric scaling. In a comparison with RHIC data in Au + Au collisions at $\sqrt{s_{NN}} = 62.4$ GeV and 200 GeV the gradual approach to the gluon saturation regime is investigated. Predictions for net-baryon rapidity spectra and the mean rapidity loss in central Pb + Pb collisions at LHC energies of $\sqrt{s_{NN}} = 5.52$ TeV are made.

DOI: 10.1103/PhysRevLett.102.182301 PACS numbers: 24.85.+p, 12.38.Mh, 25.75.Dw

Baryon stopping in relativistic heavy-ion collisions as a probe of QCD-matter at high parton density is of great current interest [1–4]. Theoretical QCD-based approaches usually focus on charged-hadron production. In the central rapidity region a reasonable understanding has been achieved in the color glass condensate framework [5–8] through inclusive gluon production [9,10]. In this theory, due to the self-interaction of gluons, the number of gluons in the nuclear wave function increases with increasing energy and decreasing longitudinal momentum fraction x carried by the parton.

Unitarity requires that the gluon density saturates below a characteristic momentum scale, the so-called saturation scale Q_s. In this regime gluons form a coherent state. Presently the evidence for the existence of this state of matter is, however, not yet clear. Because of the dependence of the saturation scale on rapidity and mass number, it has been proposed that saturation effects should be studied with heavy nuclei and large rapidities at Relativistic Heavy-Ion Collider (RHIC) energies and beyond.

In this Letter we suggest using the rapidity distribution of net baryons ($B - \bar{B}$) in central heavy-ion collisions as a testing ground for saturation physics, cf. Fig. 1. In $A + A$ collisions, two distinct and symmetric peaks with respect to rapidity y occur at Super Proton Synchrotron (SPS) energies [11] and beyond. The rapidity separation between the peaks increases with energy, and decreases with increasing mass number A reflecting larger baryon stopping for heavier nuclei, as has been investigated phenomenologically in the relativistic diffusion model [12].

The net-baryon number is essentially transported by valence quarks that probe the saturation regime in the target by multiple scatterings [13]. During the collision the fast valence quarks in one nucleus scatter in the other nucleus by exchanging soft gluons, leading to their redistribution in rapidity space. We take advantage of the fact that the valence quark parton distribution is well known at large x, which corresponds to the forward and backward rapidity region, to access the gluon distribution at small x in the target nucleus. Therefore, this picture provides a clean probe of the unintegrated gluon distribution $\varphi(x, p_T)$ at small x in the saturation regime. Here p_T is the transverse momentum transfer.

We have two symmetric contributions, coming from the two beams. The contribution of the fragmentation of the valence quarks in the forward moving nucleus is given by the simple formula [14] for the rapidity distribution of hadrons:

$$\frac{dN}{dy} = \frac{C}{(2\pi)^2} \int \frac{d^2 p_T}{p_T^2} x_1 q_v(x_1, Q_f) \varphi(x_2, p_T), \qquad (1)$$

where $x_1 = p_T/\sqrt{s}\exp(y)$, $x_2 = p_T/\sqrt{s}\exp(-y)$ are the longitudinal momentum fractions carried, respectively, by the valence quark in the projectile and the soft gluon in the target. The factorization scale is set equal to the transverse momentum, $Q_f \equiv p_T$. The contribution of valence quarks in the other beam nucleus is added incoherently by changing $y \to -y$. The gluon distribution is related to the forward dipole scattering amplitude $\mathcal{N}(x, r_T)$, for a quark dipole of transverse size r_T, through the Fourier transform

$$\varphi(x, p_T) = 2\pi p_T^2 \int r_T dr_T \mathcal{N}(x, r_T) J_0(r_T p_T). \qquad (2)$$

In the fragmentation region of the projectile the valence quark parton distribution function (PDF) is dominated by large values of x_1. We integrate out the fragmentation function such that the hadron rapidity distribution is proportional to the parton distribution. The overall constant C depends on the nature of the produced hadron.

One important prediction of the color glass condensate theory is geometric scaling: the gluon distribution depends on x and p_T only through the scaling variable $p_T^2/Q_s^2(x)$, where $Q_s^2(x) = A^{1/3} Q_0^2 x^{-\lambda}$, A is the mass number, and Q_0 sets the dimension. This has been confirmed experimentally at HERA [15]. The fit value $\lambda = 0.2$–0.3 agrees with theoretical estimates based on next-to-leading-order

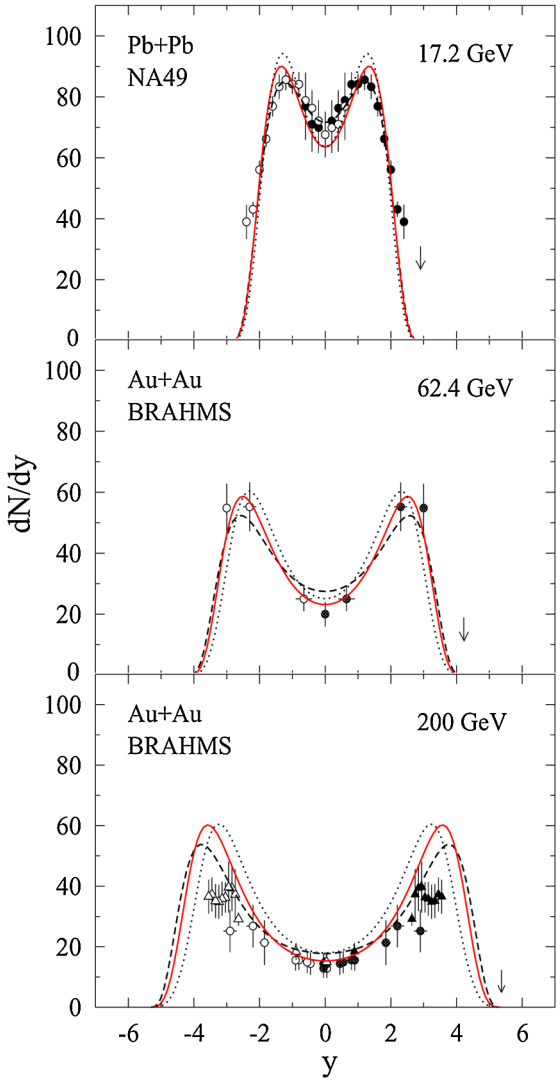

FIG. 1 (color online). Rapidity distribution of net baryons in central [(0–5)%] Pb + Pb collisions at SPS energies of $\sqrt{s_{NN}} =$ 17.2 GeV (top frame). The theoretical calculations are compared with NA49 results that have been extrapolated from the net-proton data [11]. Dashed curves are for $\lambda = 0$ and $Q_0^2 =$ 0.08 GeV^2, solid curves are for $\lambda = 0.15$ and $Q_0^2 =$ 0.07 GeV^2, and dotted curves are for $\lambda = 0.3$ and $Q_0^2 =$ 0.06 GeV^2. At RHIC energies of $\sqrt{s_{NN}} = 62.4$ GeV [middle frame, (0–10)%] and 200 GeV for central Au + Au, our corresponding theoretical results are compared with BRAHMS net-baryon data (circles) [1,2]. At 200 GeV, triangles are preliminary scaled BRAHMS net-proton data points for (0–10)% [20].

Balitskii-Fadin-Kuraev-Lipatov (BFKL) results [16,17]. To show that the net-baryon distribution reflects the geometric scaling of the gluon distribution, we perform the following change of variables:

$$x \equiv x_1, \qquad x_2 \equiv xe^{-2y}, \qquad p_T^2 \equiv x^2 s e^{-2y}. \tag{3}$$

Thus, we rewrite Eq. (1) as

$$\frac{dN}{dy}(\tau) = \frac{C}{2\pi}\int_0^1 \frac{dx}{x} x q_v(x)\varphi(x^{2+\lambda}e^{\tau}), \tag{4}$$

where $\tau = \ln(s/Q_0^2) - \ln A^{1/3} - 2(1+\lambda)y$ is the corresponding scaling variable. Hence, the net-baryon multiplicity in the peak region is only a function of a single scaling variable τ, which relates the energy dependence to the rapidity and mass number dependence. In the fragmentation region, the valence quark distribution is only very weakly dependent on Q_f.

From the equation for the isolines, $\tau =$ const, one gets the evolution of the position of the fragmentation peak in the forward region with respect to the variables of the problem

$$y_{\text{peak}} = \frac{1}{1+\lambda}(y_{\text{beam}} - \ln A^{1/6}) + \text{const}, \tag{5}$$

where $y_{\text{beam}} = 1/2 \ln[(E + p_L)/(E - p_L)] \simeq \ln\sqrt{s}/m$ is the beam rapidity at beam energy E and longitudinal momentum p_L with the nucleon mass m.

To take into account saturation effects in the target we choose the Golec-Biernat-Wüsthoff model [18] for the forward dipole scattering amplitude $\mathcal{N}$, leading to [cf. Eq. (2) and Ref. [14]]

$$\varphi(x, p_T) = 4\pi \frac{p_T^2}{Q_s^2(x)} \exp\left(-\frac{p_T^2}{Q_s^2(x)}\right). \tag{6}$$

The valence quark parton distribution of the nucleus is taken to be equal to the valence quark PDF in a nucleon times the number of participants in the nucleus. We are focusing here on the forward rapidity region, and interpolate to midrapidity where small-x quarks are dominant, by matching the leading-order distributions [19] and the Regge trajectory, $xq_v \propto x^{0.5}$, at $x = 0.01$ [3].

To account for large-x effects in the gluon distribution, we multiply the distribution function by $(1 - x_2)^4$ [10]. Mass effects are considered through the replacement $p_T \rightarrow \sqrt{p_T^2 + m^2}$.

Our results for net-baryon rapidity distributions in central Pb + Pb and Au + Au collisions are shown in Fig. 1. Dashed curves are for $\lambda = 0$, solid curves for $\lambda = 0.15$, and dotted curves for $\lambda = 0.3$, with the corresponding Q_0^2 values fixed at SPS, as given in the caption.

We compare with SPS NA49 Pb + Pb results at $\sqrt{s_{NN}} =$ 17.2 GeV [11], and BRAHMS Au + Au data at 62.4 and 200 GeV [1,2,20]. We obtain the number of baryon participants at SPS energy in the full rapidity range from a double-Gaussian fit of the NA49 data for (0–5)% central Pb + Pb collisions as $N_B = 380$. The normalization in our model calculation is 12% lower than this value since we do not account for the baryons near y_{beam} in the tails. We maintain this correction at RHIC energies where the tails are in the unmeasured region.

For Au + Au at RHIC energies, we take Glauber results for the number of participants: At 62.4 GeV $N_B = 314 \pm 8$

for centrality (0–10)% [2], and at 200 GeV $N_B = 357 \pm 8$ for (0–5)% [1]. The comparison with the SPS and RHIC data slightly favors $\lambda \leq 0.15$ and hence, the asymptotic regime with $\lambda \simeq 0.3$ is not yet reached at RHIC.

Our prediction for central Pb + Pb at 5.52 TeV LHC energies is shown in Fig. 2 for $\lambda = 0$, 0.15, and 0.3. At LHC energies the midrapidity region is almost baryon free, we obtain $dN/dy(y = 0) \simeq 4$ for net baryons. The position of the fragmentation peak is very sensitive to the value of λ, with a difference of about 1.5 units of rapidity between the $\lambda = 0$ and 0.3 cases. It is possible that the full scaling regime with λ approaching 0.3 can be reached at or beyond LHC energies, but presently none of the LHC experiments are capable of measuring identified protons or neutrons from central Pb + Pb collisions in the region of the fragmentation peaks. This would be a relevant proposal for future extensions of the detector capabilities at LHC.

Physically, the two peaks represent the result of the scattering of the fast moving projectile valence quarks in the target, they are deflected, their distribution broadens and carries information about the gluon distribution in the target. This is in analogy to x rays that are deflected by a crystal and carry information about its structure.

With increasing energy the peaks move apart, the solutions behave like traveling waves in rapidity space [21], which can be probed experimentally at distinct values of the beam energy, or the corresponding beam rapidity. We have derived the peak position as a function of the beam rapidity as $y_{\text{peak}} = \upsilon y_{\text{beam}} + \text{const}$ with the peak velocity $\upsilon = 1/(1 + \lambda)$, cf. Eq. (5). The position of the peak in rapidity space as a function of the beam energy can in principle be determined experimentally, or at least estimated (RHIC). Theoretically, its evolution with energy provides a measure of the saturation-scale exponent λ. Hence, a precise determination of the net-proton fragmentation peak position as a function of beam energy would provide detailed information about the gluon saturation scale.

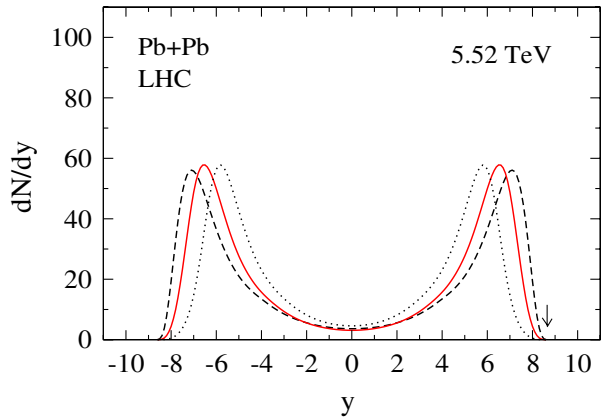

FIG. 2 (color online). Rapidity distribution of net baryons in central Pb + Pb collisions at LHC energies of $\sqrt{s_{NN}} = 5.52$ TeV. Theoretical distributions are shown for $\lambda = 0$ (dashed), $\lambda = 0.15$ (solid), and $\lambda = 0.3$ (dotted curve), with Q_0^2—values as in Fig. 1.

In Fig. 3, we show our numerical results for the mean rapidity loss $\langle \delta y \rangle = y_{\text{beam}} - \langle y \rangle$. At low energies they agree with the experimental values of baryon stopping that have been obtained at AGS and SPS energies [11,22] irrespective of the value of λ. Here we have considered the effect of the missing particles in the tails as described above for the rapidity distributions, placing them halfway between the mean rapidity and the beam value. At RHIC energies of 62.4 and 200 GeV, the mean rapidity loss depends on λ, and the $\lambda = 0.3$ result (dotted curve) is beyond the upper limit given by BRAHMS [1,2], whereas $\lambda \leq 0.15$ is consistent with the upper limit of the data. Consequently, up to the highest RHIC energies the expected scaling regime with $\lambda \simeq 0.3$ [15] is not yet fully reached, in accordance with [10,23].

Our result emphasizes the importance of a detailed measurement at LHC energies to allow more definite conclusions about the value of λ, which would then be determined by the slope of the mean rapidity loss at high beam rapidity above RHIC (solid curve in Fig. 3).

Assuming that the mean rapidity evolves similarly to the peak position, $\langle y \rangle \equiv y_{\text{peak}} + \text{const.}$, the linear increase of the mean rapidity loss at large energies corresponding to beam rapidities $y_{\text{beam}} > 5$ is given by

$$\langle \delta y \rangle = \frac{\lambda}{1 + \lambda} y_{\text{beam}} + \text{const.} \tag{7}$$

Hence, the mean rapidity loss that accompanies the energy loss in the course of the slowdown of baryons provides at large beam rapidities $y_{\text{beam}} > 5$ a measure for λ and thus, a

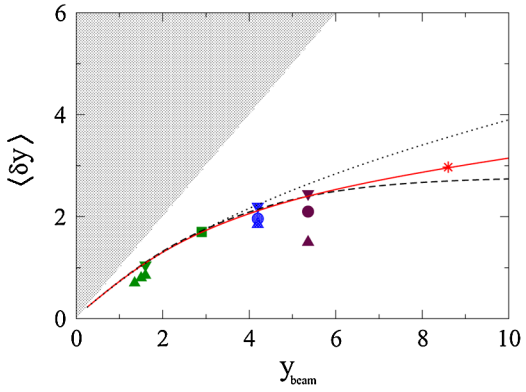

FIG. 3 (color online). The mean rapidity loss $\langle \delta y \rangle$ as obtained from our theoretical results is plotted as a function of beam rapidity y_{beam}, solid curve. The star at $y_{\text{beam}} = 8.68$ is our prediction for central Pb + Pb at LHC energies of $\sqrt{s_{NN}} = 5.52$ TeV with $\lambda = 0.15$, the dashed curve is for $\lambda = 0$, the dotted curve is for $\lambda = 0.3$, with Q_0^2 values as in Fig. 1. Analysis results from AGS Au + Au data (E917, E802/E866, triangles) [22], SPS Pb + Pb data (NA49, square) [11], RHIC Au + Au data (BRAHMS, dots, with triangles as lower and upper limits) [1,2] are compared with the calculations.

test of saturation physics. The case $\lambda = 0$, or equivalently Q_s constant, leads to a saturation of the mean rapidity loss at high energies, and correspondingly at large beam rapidities.

In the peak region, the average x in the projectile is $x \simeq 0.2$–0.3, which corresponds to the average momentum fraction carried by a valence quark. In the target, $x = (0.2\text{–}0.3)e^{-2y_{\text{peak}}}$, it decreases with increasing energy. In this kinematic regime we have a natural intrinsic hard momentum, the saturation scale Q_s. This justifies the use of small-coupling techniques in QCD for calculating integrated yields [24]. The effects of the medium are expected to be small at forward rapidity since the fast moving valence quarks escape the interaction zone quickly. A detailed measurement of the peak region would then enable us to reconstruct the gluon distribution from Eq. (1).

To summarize, we have presented a saturation model for net-baryon distributions to investigate the gradual approach to the gluon saturation regime at RHIC energies and beyond. In a comparison with BRAHMS net-baryon results for central Au + Au collisions at 62.4 and 200 GeV we have determined a saturation-scale exponent $\lambda \leq 0.15$ and hence, the full scaling regime is not yet reached at RHIC. This result is in agreement with studies of particle production that point out a slower growth of the saturation scale at RHIC energies than the HERA estimate of $\lambda \simeq 0.3$ suggests [10,23].

In particular, we have shown that the peak position in net-proton rapidity distributions of centrally colliding heavy ions at ultrarelativistic energies obeys a scaling law involving the atomic mass and the beam energy. Our result for the mean rapidity loss in $\sqrt{s_{NN}} = 62.4$ GeV and 200 GeV Au + Au is for $\lambda \leq 0.15$ consistent with the upper limit of the corresponding BRAHMS experiments. We emphasize the importance of a detailed analysis at LHC energies.

One of the authors (Y. M.-T.) acknowledges critical comments by Jamal Jalilian-Marian and Mark Strikman. We are grateful to the BRAHMS Collaboration for their data. This work has been supported by the Deutsche Forschungsgemeinschaft under Grant No. STA 509/1-1, and by the ExtreMe Matter Institute EMMI.

[1] I. G. Bearden *et al.* (BRAHMS Collaboration), Phys. Rev. Lett. **93**, 102301 (2004).

[2] H. H. Dalsgaard *et al.* (BRAHMS Collaboration), Int. J. Mod. Phys. E **16**, 1813 (2007); I. C. Arsene *et al.* (BRAHMS Collaboration), arXiv:0901.0872 [Phys. Lett. B (to be published)].

[3] K. Itakura, Y. V. Kovchegov, L. D. McLerran, and D. Teaney, Nucl. Phys. **A730**, 160 (2004).

[4] J. L. Albacete, Y. V. Kovchegov, and K. Tuchin, Nucl. Phys. **A781**, 122 (2007).

[5] L. V. Gribov, E. M. Levin, and M. G. Ryskin, Phys. Rep. **100**, 1 (1983); A. H. Mueller and J. Qiu, Nucl. Phys. **B268**, 427 (1986); J. P. Blaizot and A. H. Mueller, Nucl. Phys. **B289**, 847 (1987); L. McLerran and R. Venugopalan, Phys. Rev. D **49**, 2233 (1994).

[6] I. Balitsky, Nucl. Phys. **B463**, 99 (1996); Y. V. Kovchegov, Phys. Rev. D **60**, 034008 (1999).

[7] J. Jalilian-Marian, A. Kovner, A. Leonidov, and H. Weigert, Nucl. Phys. **B504**, 415 (1997); J. Jalilian-Marian, A. Kovner, and H. Weigert, Phys. Rev. D **59**, 014015 (1998); J. Jalilian-Marian, A. Kovner, A. Leonidov, and H. Weigert, Phys. Rev. D **59**, 034007 (1999); **59**, 099903(E) (1999).

[8] E. Iancu, A. Leonidov, and L. D. McLerran, Nucl. Phys. **A692**, 583 (2001); Phys. Lett. B **510**, 133 (2001).

[9] D. Kharzeev, E. Levin, and M. Nardi, Nucl. Phys. **A730**, 448 (2004); Nucl. Phys. **A747**, 609 (2005).

[10] J. L. Albacete, Phys. Rev. Lett. **99**, 262301 (2007).

[11] H. Appelshäuser *et al.* (NA49 Collaboration), Phys. Rev. Lett. **82**, 2471 (1999).

[12] G. Wolschin, Eur. Phys. J. A **5**, 85 (1999); Europhys. Lett. **47**, 30 (1999); **74**, 29 (2006); Phys. Rev. C **69**, 024906 (2004); Prog. Part. Nucl. Phys. **59**, 374 (2007).

[13] S. A. Bass, B. Müller, and D. K. Srivastava, Phys. Rev. Lett. **91**, 052302 (2003).

[14] D. Kharzeev, Y. V. Kovchegov, and K. Tuchin, Phys. Lett. B **599**, 23 (2004); R. Baier, Y. Mehtar-Tani, and D. Schiff, Nucl. Phys. **A764**, 515 (2006); A. Dumitru, A. Hayashigaki, and J. Jalilian-Marian, Nucl. Phys. **A765**, 464 (2006).

[15] A. M. Stasto, K. Golec-Biernat, and J. Kwieciński, Phys. Rev. Lett. **86**, 596 (2001).

[16] L. N. Lipatov, Sov. J. Nucl. Phys. **23**, 338 (1976); E. A. Kuraev, L. N. Lipatov, and V. S. Fadin, Sov. Phys. JETP **45**, 199 (1977); I. I. Balitskii and L. N. Lipatov, Sov. J. Nucl. Phys. **28**, 822 (1978).

[17] D. N. Triantafyllopoulos, Nucl. Phys. **B648**, 293 (2003).

[18] K. Golec-Biernat and M. Wüsthoff, Phys. Rev. D **59**, 014017 (1998).

[19] A. D. Martin, R. G. Roberts, W. J. Stirling, and R. S. Thorne, Phys. Lett. B **531**, 216 (2002).

[20] R. Debbe *et al.* (BRAHMS Collaboration), J. Phys. G **35**, 104004 (2008).

[21] S. Munier and R. Peschanski, Phys. Rev. Lett. **91**, 232001 (2003); Phys. Rev. D **69**, 034008 (2004).

[22] F. Videbaek and O. Hansen, Phys. Rev. C **52**, 2684 (1995); L. Ahle *et al.* (E802 Collaboration/Experiment E-866), Phys. Rev. C **60**, 064901 (1999); B. B. Back *et al.* (E917 Collaboration), Phys. Rev. Lett. **86**, 1970 (2001).

[23] T. Hirano and Y. Nara, Nucl. Phys. **A743**, 305 (2004).

[24] A. Dumitru, L. Gerland, and M. Strikman, Phys. Rev. Lett. **90**, 092301 (2003).